Probability of Excessive Hydraulic Flow through Soil Liners

Gordon A. Fenton, M.ASCE[1]; Rukhsana Liza[2]; Craig B. Lake[3]; and D. V. Griffiths, F.ASCE[4]

Abstract: Liner systems are increasingly being used to protect the environment from contaminated waste. At the same time, society is increasingly insisting on estimates of the probability that these liner systems will fail to achieve their design objectives, one of which is to limit hydraulic flow from the contaminated region to acceptably small levels. This paper presents a methodology to estimate the probability of excessive hydraulic flow, considering the spatial variability of the soil composing the liner (its mean, variance, and correlation length) as well as the liner thickness. Semiempirical equations predicting the mean and variance of the effective hydraulic conductivity of the liner, based on theory and calibrated by random finite-element method simulations, are presented and used to investigate the probability that a liner exceeds regulatory hydraulic flow requirements. The proposed methodology is illustrated by an example. **DOI: 10.1061/(ASCE)GT.1943-5606.0000817.** © *2013 American Society of Civil Engineers.*

CE Database subject headings: Waste management; Clay liners; Hydraulic conductivity; Risk management; Finite element method; Probability.

Author keywords: Waste containment; Soil liners; Effective hydraulic conductivity; Risk assessment; Reliability-based design; Spatial variability; Random finite-element method.

Introduction

Waste containment facilities rely on liner systems placed between the waste facility and the underlying aquifer to minimize contaminant migration and thereby to limit the contamination of the surrounding soil and groundwater. These liner systems may be either naturally occurring or constructed and may be comprised of various materials of various areal extents and thicknesses. Traditionally, the equation governing the total advective flow rate, Q, through a saturated soil liner is given by Darcy's law as follows:

$$Q = k_{\text{eff}} iA \tag{1}$$

where k_{eff} = effective hydraulic conductivity of the liner, i = hydraulic gradient across the liner, and A = plan area of the liner. The effective hydraulic conductivity, k_{eff}, is defined to be the uniform (i.e., spatially constant) hydraulic conductivity value, which gives the same total flow rate, Q, as that through the actual hydraulic conductivity field, k, which varies randomly with spatial position x (see, e.g., Bogardi et al. 1990). Although the flow is fully three-dimensional (3D) in this study, the hydraulic conductivity is assumed to be isotropic, such that the directional conductivities at a point are all equal to k (or to k_{eff}).

[1]Professor, Dept. of Engineering Mathematics, Dalhousie Univ., Halifax, NS, Canada B3J 1Y9; formerly, Visiting Professor, Faculty of Civil Engineering and Geosciences, Delft Univ. of Technology, 2628 CN Delft, Netherlands (corresponding author). E-mail: Gordon.Fenton@dal.ca

[2]Graduate Student, Dept. of Civil and Resource Engineering, Dalhousie Univ., Halifax, NS, Canada B3H 4R2. E-mail: rk962901@dal.ca

[3]Associate Professor, Dept. of Civil and Resource Engineering, Dalhousie Univ., Halifax, NS, Canada B3H 4R2. E-mail: Craig.Lake@dal.ca

[4]Professor, Division of Engineering, Colorado School of Mines, Golden, CO 80401-1887. E-mail: D.V.Griffiths@mines.edu

Note. This manuscript was submitted on January 20, 2012; approved on August 8, 2012; published online on August 20, 2012. Discussion period open until November 1, 2013; separate discussions must be submitted for individual papers. This paper is part of the ***Journal of Geotechnical and Geoenvironmental Engineering***, Vol. 139, No. 6, June 1, 2013. ©ASCE, ISSN 1090-0241/2013/6-937–946/$25.00.

Hydraulic conductivity is a spatially variable property, both in natural soils (Byers and Stephens 1983; Freeze and Cherry 1979) and in compacted soil liners (Rogowski et al. 1985; Benson 1993), which means that there is always some risk that the flow through a soil liner will exceed the societally acceptable maximum regulatory limit. Because k is spatially variable and random, the value of k_{eff} used in Eq. (1) is also random and is some sort of average of k. The goals of this paper are to estimate the distribution of k_{eff} and use this to estimate the probability that the total flow through the liner will exceed the regulatory limit, henceforth referred to as the exceedance probability.

Several researchers have published information relating to estimating k_{eff}. In one of the earliest works on this topic, Warren and Price (1961) used Monte Carlo simulation to study flow across a 3D cube and found k_{eff} to be the geometric average, k_G, of k (for details about the arithmetic, geometric, and harmonic averages, see Fenton and Griffiths 2008). Bouwer (1969) and Smith and Freeze (1979) all found that k_{eff} was described well by k_G for two-dimensional (2D) flow. One of the earliest attempts to analytically define k_{eff} was presented by Gutjahr et al. (1978), who used a spectral perturbation method to determine k_{eff} for an unbounded domain under uniform gradient. Gutjahr et al. (1978) proposed the following expressions for the mean of k_{eff} for 2D flow [Eq. (2)] and 3D flow [Eq. (3)]:

$$\mu_{k_{\text{eff}}} = \exp\{\mu_{\ln k}\} \tag{2}$$

$$\mu_{k_{\text{eff}}} = \exp\{\mu_{\ln k}\}\left(1 + \sigma^2_{\ln k}/6\right) \tag{3}$$

where $\mu_{\ln k}$ and $\sigma^2_{\ln k}$ = mean and variance of $\ln k$, respectively, which are obtained from the mean, μ_k, and variance, σ^2_k, of k through the transformations

$$\sigma^2_{\ln k} = \ln\left(1 + v_k^2\right) \tag{4a}$$

$$\mu_{\ln k} = \ln(\mu_k) - \frac{1}{2}\sigma^2_{\ln k} \tag{4b}$$

where $v_k = \sigma_k/\mu_k$ = coefficient of variation of k. If k is lognormally distributed, as will be assumed here, then $\exp\{\mu_{\ln k}\}$ is its median.

Using a self-consistent model, Dagan (1979) provided upper and lower bounds on the estimates of $\mu_{k_{\text{eff}}}$ in an unbounded 3D domain. His best estimate of $\mu_{k_{\text{eff}}}$ is only slightly larger than that provided by Gutjahr et al. (1978) in Eq. (3). At $\sigma_{\ln k} = 1.0$ (i.e., $v_k = 1.7$), Dagan's bounds are approximately $0.1\exp\{\mu_{\ln k}\} \leq \mu_{k_{\text{eff}}} \leq 10\exp\{\mu_{\ln k}\}$, which is a very wide range (i.e., two orders of magnitude), suggesting that there is very little confidence in analytical estimates of $\mu_{k_{\text{eff}}}$ in three dimensions.

Analysis of flow through an unbounded (i.e., infinite) domain involves the implicit assumption that the correlation length is zero because only the ratio of the correlation length to the domain size matters when it comes to spatial variability. This simplifies the theory because it results in a white noise random process where every point in the field is independent of every other point. As far as the authors are aware, soils always demonstrate some degree of spatial dependence; thus, such white noise processes are unrealistic. In other words, estimates of k_{eff} in bounded domains with nonzero correlation lengths are more useful in practice.

For a bounded (i.e., finite) domain, the influence of the liner aspect ratio (ratio of the liner's thickness to its plan dimension) on the distribution of k_{eff} was investigated by Liza (2010). Here, the liner aspect ratio will be defined to be $\xi = X/\sqrt{YZ}$, where the liner has thickness X and planar dimensions $Y \times Z$. The generality that this definition suggests has not been confirmed. Only the case where $Y = Z$ is considered here (i.e., a square liner), such that effectively $\xi = X/Y = X/Z$ in this study. The authors believe that $\xi = X/\sqrt{YZ}$ can be used even if $Y \neq Z$; however, the limits of such a belief require further investigation.

As ξ approaches zero (i.e., the liner thickness approaches zero), the total flow through the liner becomes the arithmetic sum of the flows through each point in the plane of the liner. In this case, k_{eff} becomes the arithmetic average, k_A, of k over the liner area (analogous to a set of resistors in parallel) and $\mu_{k_{\text{eff}}} = \mu_k$. Alternatively, as ξ approaches infinity (i.e., flow through a long pipe), k_{eff} approaches the harmonic average, k_H, of k. Flow through a pipe is controlled by the lowest conductivity regions encountered in the pipe, analogous to a set of resistors in series (see Fenton and Griffiths 1993). In general, k_H is the most strongly low conductivity dominated average; i.e., $k_H < k_G < k_A$.

For aspect ratios somewhere between zero and infinity, k_{eff} lies somewhere between k_A and k_H. As the liner thickness increases from zero (arithmetic average), spatial variation through the liner thickness leads to low conductivity regions that attempt to block the flow (harmonic average). However, because the flow can seek higher conductivity paths around the low conductivity regions in two or three dimensions (Benson and Daniel 1994a), k_{eff} is not as low as predicted by k_H. Fenton and Griffiths (1993) used the random finite-element (FE) method (RFEM) to examine the influence of correlation length and aspect ratio on the distribution of k_{eff} in a 2D bounded domain. For a square domain, they found k_{eff} to be equal to k_G, which is in agreement with the studies by Gutjahr et al. (1978) and Dagan (1979) in the limit when the correlation length is set to zero (unbounded domain).

In three dimensions, the best estimate of $\mu_{k_{\text{eff}}}$ is given by Eq. (3) for unbounded domains (with considerable uncertainty). For bounded domains, Eq. (3) clearly cannot generally be true. To understand why this is so, the random field model used here must first be described. In this paper, k will be assumed to be lognormally distributed so that $\ln k(x)$ is normally distributed. The $\ln k$ field is fully specified by three quantities; i.e., its mean ($\mu_{\ln k}$), its standard deviation ($\sigma_{\ln k}$), and its correlation structure (the correlation coefficient between any two points in the field). A Markovian correlation structure will be assumed here (see Vanmarcke 1984) with a separable correlation function (which is a product of the directional correlation functions) as follows:

$$\rho_{\ln k}(\tau_1, \tau_2, \tau_3) = \exp\{-2|\tau_1|/\theta_1\}\exp\{-2|\tau_2|/\theta_2\}\exp\{-2|\tau_3|/\theta_3\} \tag{5}$$

where τ_i = distance between two points in the field in each coordinate direction, $i = 1, 2$, and 3.

The decay rate parameters θ_i, for $i = 1, 2$, and 3, are the directional correlation lengths. In this study, the correlation lengths are assumed to be equal; i.e., $\theta_1 = \theta_2 = \theta_3 = \theta_{\ln k}$. Because the correlation function is separable, its corresponding variance reduction function (Vanmarcke 1984) is also separable and can be explicitly written as follows:

$$\gamma_{\ln k}(X, Y, Z) = \gamma(X)\gamma(Y)\gamma(Z) \tag{6}$$

where

$$\gamma(X) = \frac{\theta_{\ln k}^2}{2X^2}\left[\frac{2X}{\theta_{\ln k}} + \exp\left\{-\frac{2X}{\theta_{\ln k}}\right\} - 1\right] \tag{7}$$

and similarly for $\gamma(Y)$ and $\gamma(Z)$. Here, $\gamma_{\ln k}(X, Y, Z)$ will be referred to simply as $\gamma(V)$, where V represents the total liner volume (or element volume, if V is replaced by V_e).

Returning to the issue of the accuracy of Eq. (3), if the soil domain is bounded and $\theta_{\ln k} = \infty$, then every realization of the random conductivity field shows no spatial variability; i.e., all points in the field have the same (random) value, k. This statement means that $k_{\text{eff}} = k$ for each realization, and thus $\mu_{k_{\text{eff}}} = \mu_k$, which is significantly higher than suggested by Eq. (3). In other words, Eq. (3) cannot hold for bounded domains unless $\theta_{\ln k} = 0$.

The overall goal of this study is to provide semitheoretical equations allowing the simple estimation of the probability that the total flow through a liner exceeds the maximum flow prescribed by regulatory agencies. This exceedance probability can be expressed as $P[k_{\text{eff}} > k_{\text{crit}}]$, where k_{crit} is the maximum allowable regulatory hydraulic conductivity. Bogardi et al. (1990), Benson and Charbeneau (1991), and Benson and Daniel (1994a, b), have all conducted research into the reliability of soil liners where the exceedance probability is considered. However, none of these studies investigated the influence of spatial variability on exceedance probability. Menzies (2008) examined the influence of the correlation length and the distribution of k on the exceedance probability associated with flow through thin compacted soil liners, and his work agrees with the small aspect ratio (thin liner) case considered here.

To achieve the overall goal, the subsequent sections of this paper develop a prediction for the probability of exceedance as a function of the basic statistics of the random conductivity field (μ_k, σ_k, and $\theta_{\ln k}$) and the liner aspect ratio, ξ. To calibrate the prediction at intermediate aspect ratios (where the theory is not exact), simulations are performed in which the soil is divided into a set of n cubic elements and the hydraulic conductivity, k_i, assigned to the ith element is taken to be the geometric average of the random conductivity field over the ith element domain. This approach slightly underestimates the best estimate of $\mu_{k_{\text{eff}}}$ when $\theta_{\ln k} = 0$ [as in Eq. (3)] but has the correct behavior for larger $\theta_{\ln k}$. The choice of a geometric average over cubical domains is also in agreement with the work by Warren and Price (1961) and is at the center of the bounds suggested by Dagan (1979). Finally, the uses of the developed failure probability prediction equations are illustrated through an example.

Simulations

Monte Carlo simulations were performed using a 3D RFEM program, *mrflow3d*, designed to analyze stochastic fluid flow problems

J. Geotech. Geoenviron. Eng. 2013.139:937-946.

(Griffiths and Fenton 1997), which were intended to aid in the calibration of the semitheoretical failure probability equations developed subsequently in the paper. The mesh discretization used in the simulations is illustrated in Fig. 1. The cubes are shaded differently in grayscale to emphasize that they are deemed to have spatially variable hydraulic conductivities.

An impervious boundary was assumed on the vertical edges of the mesh and a uniform pressure head of 1.0 (with the same units as the liner dimensions) was applied to the upper surface of the mesh, which directs the flow downward (i.e., in the X direction on average). The inputs to the model were μ_k, σ_k, and $\theta_{\ln k}$; the number of elements in each coordinate direction; and the size of the elements. The simulation proceeded by simulating local averages, G_i, for $i = 1, 2, \ldots, n$ where n is the total number of elements in the soil model. Each local average, G_i, was the arithmetic average of a standard normal field, G, over the ith element. The final lognormally distributed hydraulic conductivity value assigned to the ith element was obtained through the transformation $k_i = \exp\{\mu_{\ln k} + \sigma_{\ln k} G_i\}$. Because G_i is an arithmetic average of G, then k_i is a geometric average of k over the ith element (Fenton and Griffiths 2008).

Flow through the model was then estimated using the FE method. As part of the analysis, k_{eff}, k_A, and k_G were calculated using the following expressions for each random field realization:

$$k_{\text{eff}} = \mu_k \left(\frac{Q}{Q_{\mu_k}} \right) \tag{8a}$$

$$k_A = \frac{1}{n} \sum_{i=1}^{n} k_i \tag{8b}$$

$$k_G = \left[\prod_{i=1}^{n} k_i \right]^{1/n} = \exp\left\{ \frac{1}{n} \sum_{i=1}^{n} \ln k_i \right\} \tag{8c}$$

where Q = total flow estimated through the current realization of the random conductivity field by the FE analysis; Q_{μ_k} = total flow through a soil having uniform hydraulic conductivity, μ_k, throughout the soil; k_i = local geometric average of the hydraulic conductivity over the ith element; and n = number of elements in the FE mesh.

Because k is assumed lognormally distributed, the mean and variance of k_G can be computed analytically to be

$$\mu_{k_G} = \exp\left\{ \mu_{\ln k} + \frac{1}{2} \gamma(V) \sigma^2_{\ln k} \right\} = \frac{\mu_k}{\left[1 + v_k^2\right]^{0.5[1-\gamma(V)]}} \tag{9a}$$

$$\sigma^2_{k_G} = \mu^2_{k_G} \left[\exp\left\{ \sigma^2_{\ln k} \gamma(V) \right\} - 1 \right] = \frac{\mu_k^2}{\left[1 + v_k^2\right]^{1-\gamma(V)}} \left[\left(1 + v_k^2\right)^{\gamma(V)} - 1 \right] \tag{9b}$$

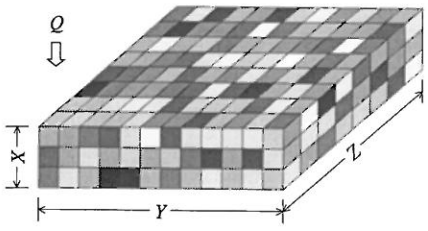

Fig. 1. Illustration of mesh discretization used in the RFEM

where $V = XYZ$ = total volume of the soil liner. The analytical computation of the mean and variance of k_A is somewhat more complicated because k_A is an arithmetic average of a series of geometric averages, k_i. The mean of k_A is given by

$$\mu_{k_A} = \exp\left\{ \mu_{\ln k} + \frac{1}{2} \gamma(V_e) \sigma^2_{\ln k} \right\} = \frac{\mu_k}{\left[1 + v_k^2\right]^{0.5[1-\gamma(V_e)]}} \tag{10a}$$

where V_e = volume of an element. Real soil liners will not have elements; thus, recommendations are made subsequently in the paper regarding what the value of V_e should be for a real soil. To compare with the simulation results, the following FE volume is used: $V_e = \Delta x \times \Delta y \times \Delta z$ where Δx, Δy, and Δz are the dimensions of each element in the FE model. Regarding the variance of k_A, it is well known that arithmetic averaging of k leads to a reduction in the variance. Unfortunately, the variance reduction function provided by Eqs. (6) and (7) gives the amount that the variance is reduced when $\ln k$ is averaged, not when k is averaged. Past experience by the authors indicate that the variance reduction in real space (averaging k) is generally quite similar to the variance reduction in log space (averaging $\ln k$) for Markov correlation structures, allowing the following approximation:

$$\sigma^2_{k_A} \simeq \gamma(V) \sigma^2_{k_i} = \frac{\gamma(V) \mu_k^2}{\left[1 + v_k^2\right]^{1-\gamma(V_e)}} \left[\left(1 + v_k^2\right)^{\gamma(V_e)} - 1 \right] \tag{10b}$$

where $\sigma^2_{k_i}$ = variance of the geometric average of k over the ith element, having volume V_e [see Eq. (9b), replacing V with V_e].

The distribution of k_{eff} can be estimated by simulation. Fig. 2 demonstrates that the frequency-density plot of k_{eff} is well fit by a lognormal distribution, having a p value of 0.84, which indicates strong support for the fit. On the basis of Fig. 2, and similar results found for other values of μ_k, v_k, $\theta_{\ln k}$, and ξ (not shown), the distribution of k_{eff} will be assumed to be lognormal. In this case, the exceedance probability, $P[k_{\text{eff}} > k_{\text{crit}}]$, is given by

$$P\left[k_{\text{eff}} > k_{\text{crit}}\right] = 1 - \Phi\left(\frac{\ln k_{crit} - \mu_{\ln k_{\text{eff}}}}{\sigma_{\ln k_{\text{eff}}}} \right) \tag{11}$$

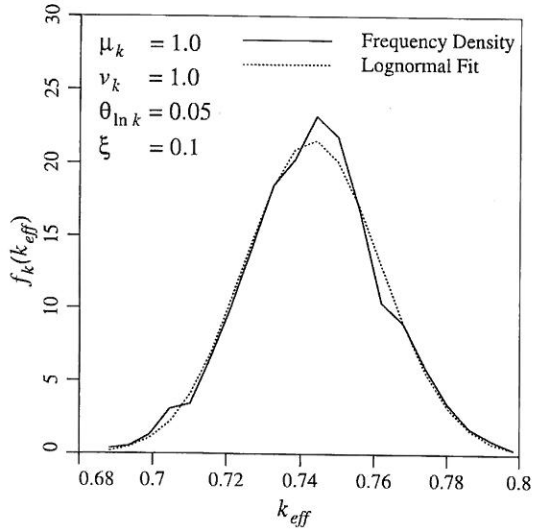

Fig. 2. Frequency-density plot of k_{eff}, based on 1,000 realizations, with fitted lognormal distribution

J. Geotech. Geoenviron. Eng. 2013.139:937-946.

where Φ = standard normal cumulative distribution function, and $\mu_{\ln k_{\text{eff}}}$ and $\sigma_{\ln k_{\text{eff}}}$ = mean and SD of $\ln k_{\text{eff}}$, respectively.

Parameters Used in the Simulations

The soil model used in the simulations (see Fig. 1) had planar dimensions $Y \times Z = 1.0 \times 1.0$. To calibrate the effect of liner thickness on exceedance probability at intermediate aspect ratios (where calibration is required), ξ was varied from 0.1 to 1.0. Smaller values of the aspect ratio represent liners used in landfills having large areal extent relative to their thickness, while larger aspect ratios (e.g., $\xi = 1.0$) correspond to liners used in small leachate lagoons or using very thick natural clay deposits. In each simulation, μ_k can be normalized with respect to the regulatory value, k_{crit}, by using μ_k/k_{crit} in place of μ_k. Here, except for the final example where real values are used, this normalization has been carried out in which $\mu_k = 1.0$ indicates that the actual mean conductivity is equal to k_{crit}.

The parametric variations considered in the simulations for a total of $n_{\text{par}} = 4 \times 3 \times 7 \times 4 = 336$ simulation runs (each of which consisted of $n_{\text{sim}} = 1{,}000$ realizations of the k field) were as follows:

- Normalized mean hydraulic conductivities: $\mu_k = 0.5, 1.0, 1.5,$ and 2.0;
- Coefficients of variation: $v_k = 0.5, 1.0,$ and 2.0;
- Correlation lengths: $\theta_{\ln k} = 0.01, 0.05, 0.1, 0.5, 1.0, 5.0,$ and 10.0; and
- Aspect ratio of liner: $\xi = 0.1, 0.3, 0.6,$ and 1.0.

Values of $\xi < 0.1$ were not considered in the simulation because the probabilistic behavior of thin liners is already known by theory.

A sensitivity analysis was performed to examine the influence of the element mesh refinement on the relative accuracy of the output quantities of interest (k_{eff}, k_A, and k_G), for the case where $\xi = 1.0$. To this end, a soil domain of size $1 \times 1 \times 1$ was discretized into $20 \times 20 \times 20$ up to $32 \times 32 \times 32$ elements. All mesh resolutions gave similar results; thus, the $20 \times 20 \times 20$ element mesh was selected for the subsequent simulation runs because it runs about 50 times faster than the $32 \times 32 \times 32$ mesh (e.g., 1 week rather than 1 year at 2011 computer speeds). The $20 \times 20 \times 20$ mesh discretization means that each element has dimensions $\Delta x \times \Delta y \times \Delta z = 0.05 \times 0.05 \times 0.05$. The correlation lengths considered in the study thus ranged from significantly less than the element size ($\theta_{\ln k} = 0.01 \ll 0.05$) to significantly larger than the soil regime ($\theta_{\ln k} = 10.0 \gg 1.0$).

The other aspect ratios considered (e.g., $\xi = 0.1$) were implemented simply by reducing the number of elements in the X direction. Thus, the mesh corresponding to $\xi = 0.1$ was of size $2 \times 20 \times 20$, and so on. Although the choice of a lower bound on the aspect ratio of 0.1 may seem questionable, smaller values are not needed because theory dictates that as $\xi \to 0$, then $k_{\text{eff}} \to k_A$. In other words, the only uncertainty in analytically predicted probabilities is at intermediate aspect ratios; therefore, only ξ ranging from 0.1 to 1.0 were considered in the simulations. It will be seen in the subsequent section that even when $\xi = 0.1$, the value of k_{eff} is very close to its limiting value of k_A, as expected by theory. The choice of a basic plan area of $Y \times Z = 1 \times 1$ allows the results to be easily scaled to any liner plan area as long as both the aspect ratio and the ratio of the correlation length to a representative plan dimension (e.g., $\sqrt{YZ}$) are maintained. The correlation length must have the same units as the dimensions of the clay layer.

All simulations involved generating 1,000 ($= n_{\text{sim}}$) realizations for each parameter set considered. This means that the standard deviations of each of the averages computed in Eq. (8) are approximately $\sigma_k/\sqrt{n_{\text{sim}}} = 0.03\sigma_k$ (based on the SD of k_A). This also means that the SD of any probability estimate is approximately $\sqrt{\hat{p}(1-\hat{p})/n_{\text{sim}}}$, where $\hat{p}$ is the estimated probability. In general, for small probabilities, the SD of the probability estimate is approximately $0.03\sqrt{\hat{p}}$, which means that this simulation cannot resolve accurate probability estimates of less than about 0.001.

Results

Mean Effective Hydraulic Conductivity

The influence of correlation length on the averages (sample means) of k_A, k_G, and k_{eff} are shown in Figs. 3 and 4 for liner aspect ratios of 0.1 and 1.0, respectively. Both Figs. 3 and 4 are based on simulation averages and indicate that, as expected by theory, when the correlation length is small all averages start at the median ($\exp\{\mu_{\ln k}\}$) and when the correlation length is large all averages approach the mean (μ_k).

For all aspect ratios considered in this study, the average of k_{eff} was found to lie between the geometric and arithmetic averages. A comparison of Fig. 3 ($\xi = 0.1$) versus Fig. 4 ($\xi = 1.0$) reveals that the average of k_{eff} approaches the arithmetic average when the aspect ratio is small, as expected. Plots of average k_{eff} versus the aspect ratio (not shown) are basically straight lines over the range of aspect ratios considered in the simulations, indicating that the following linear regression is appropriate as a prediction for the mean of k_{eff}:

$$\mu_{k_{\text{eff}}} = \alpha_\mu \xi \mu_{k_G} + (1 - \alpha_\mu \xi)\mu_{k_A} \tag{12}$$

where μ_{k_G} = mean of k_G and μ_{k_A} = mean of k_A. When $\xi \to 0$ (thin liner), $\mu_{k_{\text{eff}}} \to \mu_{k_A}$, as desired.

The regression coefficient, α_μ, is obtained by minimizing the sum of squared errors between prediction and simulation as follows:

$$\alpha_\mu = \frac{\sum_{j=1}^{n_{\text{par}}} \xi_j \left(\mu_{k_{Aj}} - \mu_{k_{Gj}}\right)\left(\mu_{k_{Aj}} - \hat{\mu}_{k_{\text{eff}j}}\right)}{\sum_{j=1}^{n_{\text{par}}} \left[\xi_j \left(\mu_{k_{Aj}} - \mu_{k_{Gj}}\right)\right]^2} = 0.7669 \tag{13}$$

where $n_{\text{par}} = 336$ = total number of parameter sets considered (see the previous section); ξ_j = aspect ratio of the jth parameter set; $\mu_{k_{Aj}}$

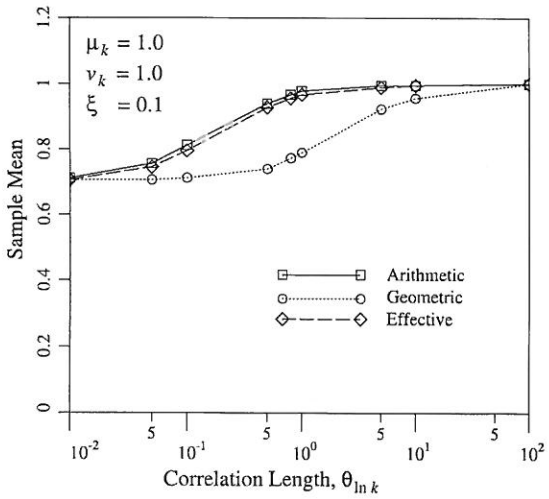

Fig. 3. Influence of correlation length on the sample means of k_A, k_G, and k_{eff} for liner aspect ratio $\xi = 0.1$

J. Geotech. Geoenviron. Eng. 2013.139:937-946.

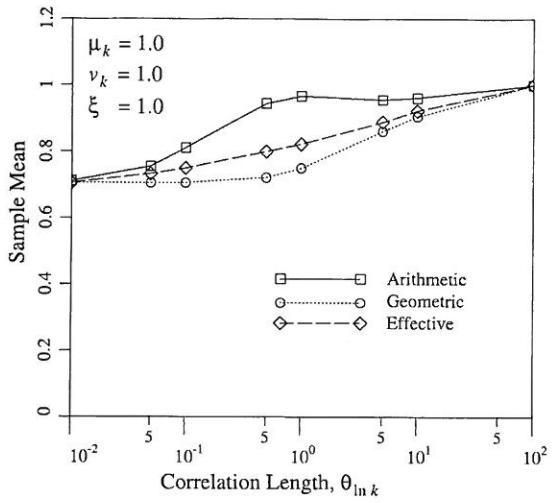

Fig. 4. Influence of correlation length on the sample means of k_A, k_G, and k_{eff} for liner aspect ratio $\xi = 1.0$

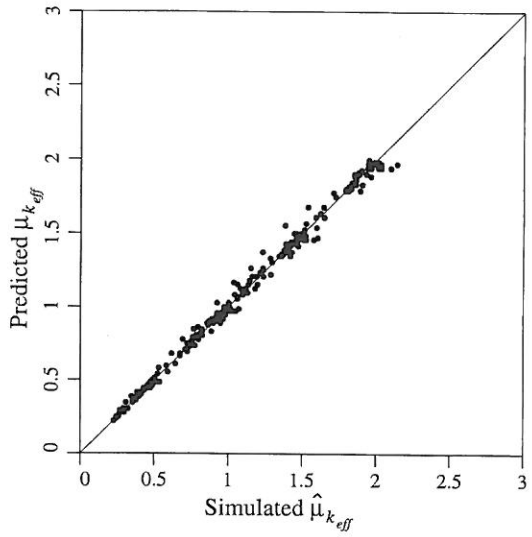

Fig. 5. Comparison of predicted mean effective hydraulic conductivity with simulated sample means

and $\mu_{k_{Gj}}$ = arithmetic and geometric means predicted for the jth parameter set [see Eqs. (9*a*) and (10*a*)], respectively; and $\hat{\mu}_{k_{\text{eff}j}}$ = sample mean k_{eff} estimated from the jth parameter set simulation run, based on 1,000 realizations. Fig. 5 shows the comparison between the simulated and predicted [Eq. (12)] mean effective hydraulic conductivity over all parameter sets. The predicted and simulated results agree very well.

SD of Effective Hydraulic Conductivity

Figs. 6 and 7 show the influence of $\theta_{\ln k}$ on the SD of k_A, k_G, and k_{eff} for aspect ratios of 0.1 and 1.0, respectively, as estimated from 1,000 realizations. Figs. 6 and 7 illustrate that as $\theta_{\ln k}$ increases, the SD of all three averages increase toward their limiting value of $\sigma_k = 1.0$, as expected by theory (Fenton and Griffiths 1993). Also, the SD of k_{eff} is very close to σ_{k_A} when $\xi = 0.1$, and approaches σ_{k_G} for larger aspect ratios.

As with the predicted mean, a linear regression of the form

$$\sigma_{k_{\text{eff}}} = \alpha_\sigma \xi \sigma_{k_G} + (1 - \alpha_\sigma \xi)\sigma_{k_A} \tag{14}$$

was found to be appropriate to predict the SD of k_{eff}. The form of Eq. (14) ensures that $\sigma_{k_{\text{eff}}} = \sigma_{k_A}$ when $\xi = 0$, as desired. The values of σ_{k_G} and σ_{k_A} are calculated using Eqs. (9*b*) and (10*b*) and the regression coefficient, α_σ, is obtained from

$$\alpha_\sigma = \frac{\sum_{j=1}^{n_{\text{par}}} \xi_j \left(\sigma_{k_{Aj}} - \sigma_{k_{Gj}}\right)\left(\sigma_{k_{Aj}} - \hat{\sigma}_{k_{\text{eff}j}}\right)}{\sum_{j=1}^{n_{\text{par}}} \left[\xi_j \left(\sigma_{k_{Aj}} - \sigma_{k_{Gj}}\right)\right]^2} = 0.9579 \tag{15}$$

where $\sigma_{k_{Aj}}$ and $\sigma_{k_{Gj}}$ = SD of the arithmetic and geometric averages predicted for the jth parameter set [see Eqs. (9*b*) and (10*b*)], respectively; and $\hat{\sigma}_{k_{\text{eff}j}}$ = sample SD of k_{eff} estimated from the jth parameter set simulation (1,000 realizations).

Fig. 8 shows the comparison between the simulated and predicted [Eq. (14)] SD of k_{eff} over all parameter sets. The predicted and simulated results agree very well; however, they show somewhat more scatter than seen in the comparison of the predicted and simulated means (Fig. 5). This result is to be expected because the uncertainty of SD estimates is higher than the uncertainty of mean estimates.

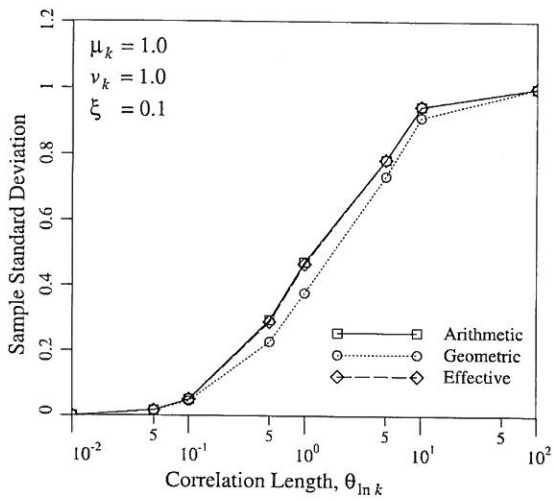

Fig. 6. Influence of correlation length on the sample SD of k_A, k_G, and k_{eff} for liner aspect ratio $\xi = 0.1$

Exceedance Probability

The exceedance probability is the probability that the effective hydraulic conductivity exceeds the regulatory hydraulic conductivity, $P[k_{\text{eff}} > k_{\text{crit}}]$. The mean and SD of k_{eff} are predicted by Eqs. (12) and (14). As demonstrated by Fig. 2, k_{eff} is lognormally distributed with the parameters given by Eq. (4*a*). Armed with these results, the probability of exceedance can be predicted using Eq. (11). Fig. 9 shows how the predicted and estimated (from simulation) exceedance probabilities compare for both the thinnest and thickest liners considered here, $\xi = 0.1$ and 1.0, and the agreement is seen to be excellent.

Fig. 10 shows that out of the 336 parameter sets considered in this study, six cases showed relatively poor agreement between predicted and simulated exceedance probabilities. These poor fits have been identified using plus signs in Fig. 10 and all six cases correspond to $\mu_k = 2.0$, $\nu_k = 2.0$, and $\theta_{\ln k} \le 0.5$. There are a total of 16 parameter set cases where $\mu_k = 2.0$, $\nu_k = 2.0$, and $\theta_{\ln k} \le 0.5$; therefore, only

J. Geotech. Geoenviron. Eng. 2013.139:937-946.

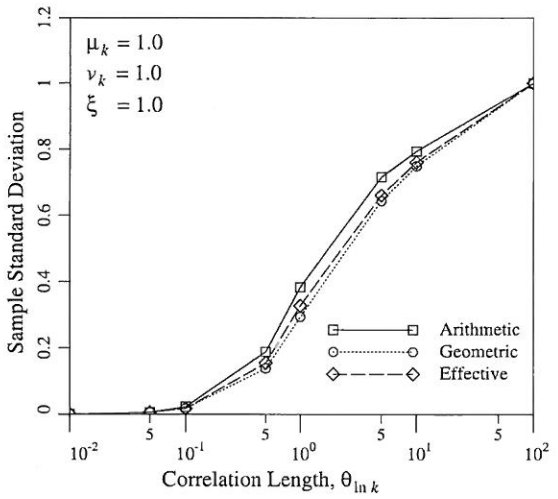

Fig. 7. Influence of correlation length on the sample SD of k_A, k_G, and k_{eff} for liner aspect ratio $\xi = 1.0$

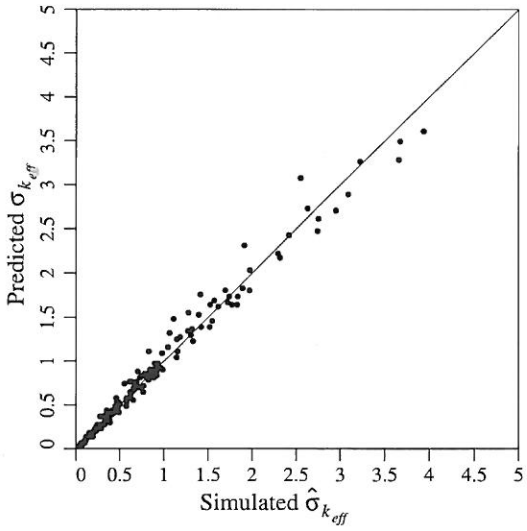

Fig. 8. Comparison of predicted SD of k_{eff} with simulated sample SD

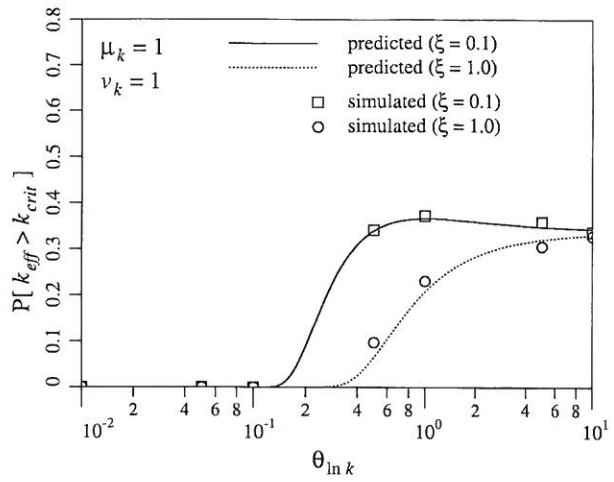

Fig. 9. Comparison of predicted and simulation-based exceedance probabilities for $\xi = 0.1$ and 1.0

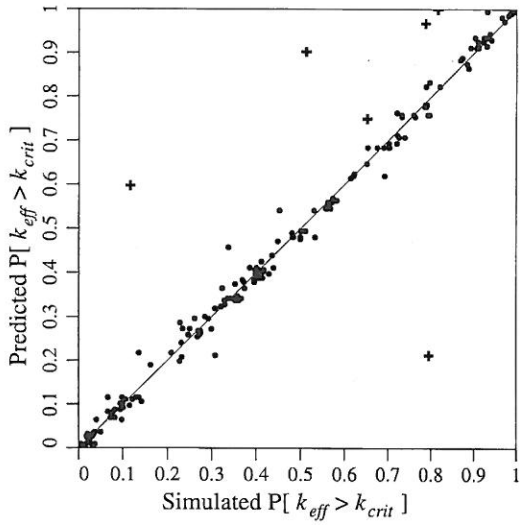

Fig. 10. Comparison of predicted and simulation-based exceedance probabilities over all parameter sets (relatively poor agreements are shown with + signs rather than dots)

about one-third of these cases actually resulted in poor agreement between simulation and prediction.

Fig. 10 suggests that the prediction of the exceedance probability provided by the semiempirical theory proposed previously is not always accurate for large υ_k and μ_k and small $\theta_{\ln k}$. For example, errors in estimates of the variance reduction, γ, become magnified when υ_k is large because all of the predictions for the means and SD of the various conductivity averages involve terms of the form $[1+\upsilon_k^2]^{1-\gamma}$. If the cases where $\mu_k \geq 2.0$ and $\upsilon_k \geq 2.0$ are omitted from consideration the agreement between predicted and simulated exceedance probabilities improves because all of the plus signs in Fig. 10 disappear. In addition, because cases where $\mu_k \geq 2.0$ generally correspond to exceedance probabilities well in excess of 50%, accurately predicting their exceedance probabilities is not so important. For practical cases, the prediction of the exceedance probability given by Eq. (11) is seen to be quite accurate and the prediction will be used subsequently to investigate the behavior of the exceedance probability with respect to the basic parameters of the random hydraulic conductivity field; i.e., $\theta_{\ln k}$, μ_k, υ_k, and ξ.

Fig. 11 shows that the exceedance probability basically decreases toward zero with decreasing correlation length for any liner thickness. The fact that the exceedance probability approaches zero at small correlation lengths is expected. That is, when the correlation length is small (e.g., $\theta_{\ln k} \leq 0.1$), the mean of all three averages shown in Figs. 3 and 4 are approaching the median, which is $\exp\{\mu_{\ln k}\} = 0.71$ when $\mu_k = 1.0$ and $\upsilon_k = 1.0$. Because this is considerably below the standardized regulatory value used in this study, $k_{\text{crit}} = 1.0$, and because the SD of all three averages become small when the correlation length is small (see Figs. 6 and 7), the probability of exceedance becomes understandably very small when $\theta_{\ln k} \to 0$, as seen in Fig. 11.

On the other hand, as $\theta_{\ln k} \to \infty$, the mean of all three averages approaches μ_k (see Figs. 3 and 4) and the SD of all three averages approaches σ_k (see Figs. 6 and 7). In other words, when $\theta_{\ln k} = \infty$ and $\mu_k = 1$ and $\sigma_k = 1$, as considered in Fig. 11, $\mu_{k_{\text{eff}}} = \mu_k = 1$ and

J. Geotech. Geoenviron. Eng. 2013.139:937-946.

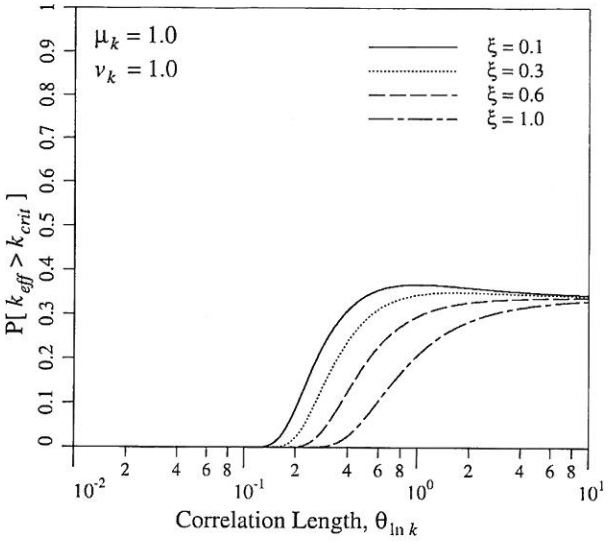

Fig. 11. Influence of correlation length and liner aspect ratio on predicted exceedance probability

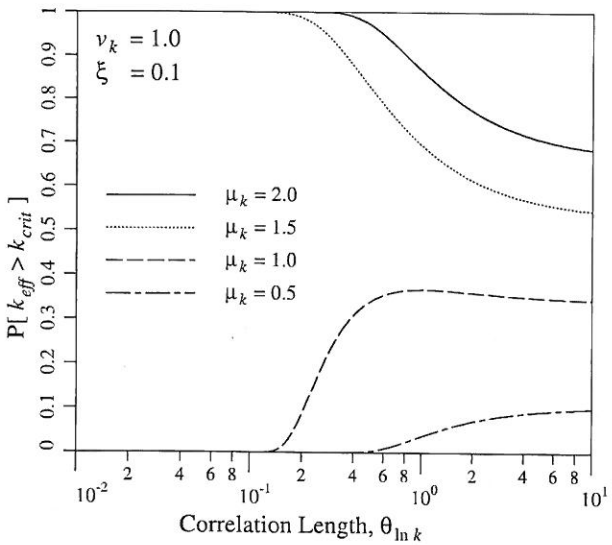

Fig. 12. Influence of correlation length and normalized mean hydraulic conductivity on predicted exceedance probability

$\sigma_{k_{\text{eff}}} = \sigma_k = 1$ are obtained such that $v_{k_{\text{eff}}} = 1/1 = 1$. The parameters of the lognormally distributed k_{eff} in this case are then $\sigma_{\ln k_{\text{eff}}} = \sqrt{\ln(1+1^2)} = 0.8326$ and $\mu_{\ln k_{\text{eff}}} = \ln(1) - (0.8326)^2 = -0.3466$; thus, according to Eq. (11)

$$P[k_{\text{eff}} > k_{\text{crit}}] = 1 - \Phi\left(\frac{0.3466}{0.8326}\right) = 0.339$$

which is what all curves in Fig. 11 are tending toward as $\theta_{\ln k} \to \infty$.

Of additional interest in Fig. 11 is the fact that a worst-case correlation length exists, where the exceedance probability reaches a maximum, for the more commonly encountered thinner liners ($\xi < 0.5$) but not for the thicker liners. When $\xi < 0.5$, the worst-case correlation length is seen to be about 50% of the plan liner dimension (e.g., $\sqrt{YZ}$). The existence of a worst-case correlation length (e.g., $\theta_{\ln k} \simeq 0.5\sqrt{YZ}$) is important because it can be conservatively used in the event that the true correlation length is unknown—and the true correlation length is almost always unknown at a site. However, the worst case does not always occur at an intermediate correlation length, as is also seen when Fig. 12 is considered. In general three worst cases should be considered ($\theta_{\ln k} \to 0$, $\theta_{\ln k} \simeq 0.5\sqrt{YZ}$, and $\theta_{\ln k} \to \infty$), to find the most conservative estimate of the exceedance probability.

Fig. 12 illustrates how the exceedance probability changes as a function of μ_k and $\theta_{\ln k}$. Recall that μ_k is normalized in this paper by k_{crit} so that k_{crit} is taken as 1.0. In general, if the mean effective hydraulic conductivity, $\mu_{k_{\text{eff}}}$, exceeds $k_{\text{crit}} = 1$, then the exceedance probability, $P[k_{\text{eff}} > k_{\text{crit}}]$, will be larger than 50%.

Consider first the limiting behavior of Fig. 12. As $\theta_{\ln k} \to 0$, k_{eff} becomes equal to the median, $\mu_{k_{\text{eff}}} = \exp\{\mu_{\ln k}\}$. When $v_k = 1.0$ and $\mu_k = 1.5$, then $\mu_{\ln k} = 0.059$ so that $\mu_{k_{\text{eff}}} = 1.06 > k_{\text{crit}}$. At the same time, the SD of the effective hydraulic conductivity, $\sigma_{k_{\text{eff}}}$, is going to zero as $\theta_{\ln k} \to 0$ (see Figs. 6 and 7), which means that $P[k_{\text{eff}} > k_{\text{crit}}] \to 1.0$. In other words, when the median of k, $\exp\{\mu_{\ln k}\}$, exceeds 1.0, the exceedance probability is near 1.0 at small correlation lengths. In this case, the worst case (highest exceedance probability) occurs when $\theta_{\ln k} \to 0$, which is as seen in Fig. 12. As the correlation length increases from zero, the exceedance probability decreases from 1.0, which is because $\sigma_{k_{\text{eff}}}$ increases rapidly with increasing $\theta_{\ln k}$ (see Figs. 6 and 7).

When the median of k is less than 1.0 (i.e., μ_k less than about 1.4 when $v_k = 1.0$), the exceedance probability starts near 0 at small correlation lengths. As the correlation length increases, both the mean and SD of k_{eff} increase, leading to an increase in the exceedance probability, as seen in Fig. 12. When $\mu_k = 0.5$, the maximum of $\mu_{k_{\text{eff}}}$ (attained when $\theta_{\ln k}$ is large) is still only half the regulatory k_{crit}. That is, when $\mu_k = 0.5$ and $v_k = 1.0$, the maximum exceedance probability, which is about 10%, occurs when $\theta_{\ln k}$ is large. In other words, when the mean hydraulic conductivity is small, relative to the regulatory value, and when $\xi > 0.3$ (see Fig. 11), the worst-case exceedance probability occurs when $\theta_{\ln k} \to \infty$; i.e., when $\mu_{k_{\text{eff}}} = \mu_k$ and $\sigma_{k_{\text{eff}}} = \sigma_k$.

Fig. 13 illustrates how the exceedance probability is influenced by the coefficient of variation, v_k. Fig. 13 presents somewhat counterintuitive results, in that as v_k increases the exceedance probability decreases. The reason for this is because at least at some level of geometric averaging, both μ_{k_A} and μ_{k_G} decrease with increasing v_k [see Eqs. (9*a*) and (10*a*)]. This means that $\mu_{k_{\text{eff}}}$ decreases with increasing v_k, resulting in the exceedance probability decreasing (see Benson and Daniel 1994b).

Estimating Probability of Exceedance: Example

The methodology presented in this paper to estimate the probability of exceedance is perhaps best illustrated through an example. Consider a proposed liner that has a plan area of 10×10 m and thickness, X, of 1 m such that $\xi = 1/\sqrt{10 \times 10} = 0.1$. While this is considered to be a very small liner, the procedure presented subsequently is identical to that required for any liner geometry. This geometry was selected because it can be compared with the simulation results carried out previously.

Suppose that testing of the clay intended to be used to construct the liner suggests that $\mu_k = 1 \times 10^{-9}$m/s, which is equal to the regulatory conductivity, $k_{\text{crit}} = 1 \times 10^{-9}$m/s, and has $v_k = 1.0$. The final constructed liner will be assumed to have a correlation length of $\theta_{\ln k} = 3$ m in all three directions (which is approximately the worst case). The desire is to quantify the probability that the actual k_{eff} will exceed the regulatory value.

One fundamental issue that first needs to be resolved is how to choose the size of the elemental geometric averaging domain. In the

J. Geotech. Geoenviron. Eng. 2013.139:937-946.

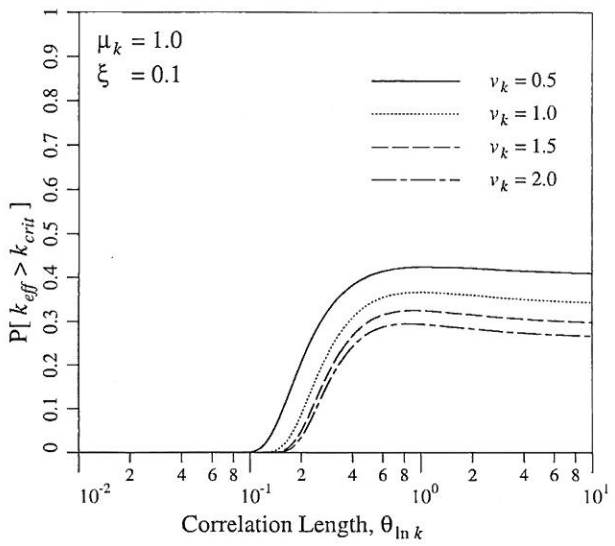

Fig. 13. Influence of correlation length and hydraulic conductivity coefficient of variation on predicted exceedance probability

previous simulations, this size was quite naturally the size of the FEs used. However, a real liner will have no preordained element size. Nevertheless, as soon as the liner thickness increases from zero, some geometric averaging will take place, as previously discussed. It is recommended here that the size of the cube over which geometric averaging takes place should be the lesser of (1) 5% of the representative plan dimension, $\sqrt{YZ}$, or (2) the liner thickness, X. In this example, $0.05\sqrt{YZ} = 0.05\sqrt{10 \times 10} = 0.5$ m, while the liner thickness is $X = 1$ m. Thus, a geometric averaging element dimension of $\Delta x = \Delta y = \Delta z = 0.5$ m was selected.

The two variance function values that are required by the method [see Eqs. (9) and (10*a*)] are $\gamma(V) = \gamma(X)\gamma(Y)\gamma(Z)$ and $\gamma(V_e) = \gamma(\Delta x)\gamma(\Delta y)\gamma(\Delta z)$, where according to Eq. (7)

$$\gamma(0.5) = \frac{3^2}{2(0.5)^2}\left[\frac{2(0.5)}{3} + \exp\left\{-\frac{2(0.5)}{3}\right\} - 1\right] = 0.8976$$

Similarly, $\gamma(1.0) = 0.8104$ and $\gamma(10.0) = 0.2551$, which according to Eq. (6) gives

$$\gamma(V_e) = \gamma^3(0.5) = 0.8976^3 = 0.7231$$

$$\gamma(V) = \gamma(1.0)\gamma(10.0)\gamma(10.0) = 0.8104(0.2551)^2 = 0.05272$$

Eqs. (9*a*) and (9*b*) can now be used to find the mean and standard deviation of the geometric average k_G

$$\mu_{k_G} = \frac{1 \times 10^{-9}}{[1+1^2]^{0.5(1-0.05272)}} = 0.7201 \times 10^{-9}\ \text{m/s}$$

$$\sigma_{k_G} = \sqrt{\frac{(1 \times 10^{-9})^2}{[1+1^2]^{1-0.05272}}\left[(1+1^2)^{0.05272} - 1\right]}$$
$$= 0.1389 \times 10^{-9}\ \text{m/s}$$

Similarly, Eq. (10*a*) can be used to find the mean and standard deviation of the arithmetic average k_A

$$\mu_{k_A} = \frac{1 \times 10^{-9}}{[1+1^2]^{0.5(1-0.7231)}} = 0.9085 \times 10^{-9}\ \text{m/s}$$

$$\sigma_{k_A} \simeq \sqrt{\frac{0.05272(1 \times 10^{-9})^2}{[1+1^2]^{1-0.7231}}\left[(1+1^2)^{0.7231} - 1\right]}$$
$$= 0.1683 \times 10^{-9}\ \text{m/s}$$

Using $\alpha_\mu = 0.7669$, as found in previously from the simulation results, the mean k_{eff} can be estimated from Eq. (12) as follows:

$$\mu_{k_{\text{eff}}} = 0.7669(0.1)(0.7201 \times 10^{-9}) + [1 - 0.7669(0.1)](0.9085 \times 10^{-9})$$
$$= 0.8940 \times 10^{-9}\ \text{m/s}$$

which is close to μ_{k_A}, as expected, because the aspect ratio of the liner is relatively small ($\xi = 0.1$). Using $\alpha_\sigma = 0.9579$ in Eq. (14) allows the estimation of the SD of k_{eff}

$$\sigma_{k_{\text{eff}}} = 0.9579(0.1)(0.1389 \times 10^{-9}) + [1 - 0.9579(0.1)](0.1683 \times 10^{-9})$$
$$= 0.1655 \times 10^{-9}\ \text{m/s}$$

such that $v_{k_{\text{eff}}} = \sigma_{k_{\text{eff}}}/\mu_{k_{\text{eff}}} = 0.1655/0.8940 = 0.1851$. Transforming into log space [Eq. (4*a*)] gives the distribution parameters of k_{eff}

$$\sigma_{\ln k_{\text{eff}}} = \sqrt{\ln(1 + 0.1851^2)} = 0.1835$$

$$\mu_{\ln k_{\text{eff}}} = \ln(0.8940 \times 10^{-9}) - \frac{1}{2}(0.1835)^2 = -20.85$$

and the final probability of exceedance estimate is obtained using Eq. (11)

$$P[k_{\text{eff}} > k_{\text{crit}}] = 1 - \Phi\left(\frac{\ln(1 \times 10^{-9}) + 20.85}{0.1835}\right)$$
$$= 1 - \Phi(0.691) = 0.241$$

In terms of the simulation, this example is equivalent to the case where $\mu_k = 1.0$, $v_k = 1.0$, $X \times Y \times Z = 0.1 \times 1.0 \times 1.0$, and $\theta_{\ln k} = 0.3$. Using these parameters, the simulation-based probability of exceedance is 0.242, which is in excellent agreement with that predicted using the theoretical approach presented previously.

Summary and Conclusions

Considering 3D spatial variability, the distribution of the liner effective hydraulic conductivity, k_{eff}, is predicted using theoretical results known at both small and large aspect ratios and correlations lengths, combined with calibration by RFEM Monte Carlo simulations at the intermediate aspect ratios and correlation lengths. The predicted distribution of k_{eff} is then used to estimate the probability that the soil liner will fail to maintain an acceptable overall level of safety with respect to hydraulic flow; i.e., to estimate the probability that k_{eff} exceeds some prescribed regulatory conductivity, $P[k_{\text{eff}} > k_{\text{crit}}]$. The paper considers only risk associated with Darcy

flow through a liner, and not, for example, with chemical transport. However, the proposed methodology can also be used to assess liner risks as a result of other liner limit states.

In estimating the mean and variance of the effective hydraulic conductivity of a liner, it was assumed that there is some elemental level over which geometric averaging of hydraulic conductivity always occurs; therefore, the arithmetic average is really an arithmetic average of geometric averages. The authors recommend that the geometric averaging element be cubic with the side dimension equal to the smaller of $0.05\sqrt{YZ}$ or the liner thickness, X. Another assumption made in the model is that the variance reduction because of arithmetic averaging of k over the liner volume is approximately equal to the variance reduction because of arithmetic averaging of $\ln k$ over the same volume. These assumptions are believed to be reasonable, although a few discrepancies between the predicted and simulated exceedance probabilities may suggest that they are inaccurate when $\mu_k \geq 2k_{\text{crit}}$ and $v_k \geq 2$. The authors note that a liner having $\mu_k \geq 2k_{\text{crit}}$ would probably be unacceptable in any case; thus, these conditions are of limited practical interest.

The following observations regarding the behavior of the distribution of k_{eff} can be made on the basis of this study:

1. The mean of k_{eff} increases from the median of $k(\exp\{\mu_{\ln k}\})$ to the mean of $k(\mu_k)$ as the correlation length increases.
2. The SD of k_{eff} increases from zero to σ_k as the correlation length increases.
3. The distribution of k_{eff} is at least approximately lognormal (see Fig. 2).
4. The distribution of k_{eff} lies between the distributions of k_A and k_G (where it is noted that k_A is actually an arithmetic average of geometric averages) and its parameters are accurately estimated by simple linear regression.

The following observations regarding the behavior of the exceedance probability can be made on the basis of this study:

1. The exceedance probability increases with increasing correlation length if the median of k is less than the regulatory conductivity, k_{crit} (the case where the median exceeds k_{crit} is of little interest because this case will almost certainly be considered unacceptable).
2. The exceedance probability increases as the liner becomes thinner (decreasing ξ).
3. The exceedance probability increases with increasing hydraulic conductivity mean, μ_k.
4. The exceedance probability decreases with increasing v_k for fixed μ_k. This possibly counterintuitive observation arises mostly because of the blocking influence of downstream variation when that variation increases in magnitude (i.e., when the low conductivity regions become even lower).
5. A worst-case correlation length is seen to exist (having the highest exceedance probability), which can be conservatively used in the event that the actual correlation length is unknown. In the cases where the median of k is less than k_{crit}, the worst case occurs when $\theta_{\ln k} \simeq 0.5\sqrt{YZ}$ for aspect ratios $\xi \leq 0.3$ and at $\theta_{\ln k} \to \infty$ for higher aspect ratios.

Acknowledgments

The authors gratefully acknowledge the financial support of the Natural Sciences and Engineering Research Council of Canada.

Notation

The following symbols are used in this paper:

A = liner plan area = $Y \times Z$;
G = standard normal random field;
G_i = local average of G over the ith element (having volume V_e);
k = spatially variable random hydraulic conductivity field;
k_A = arithmetic average of element geometric averages over the liner volume;
k_{crit} = prescribed regulatory maximum allowable hydraulic conductivity;
k_{eff} = effective hydraulic conductivity that would lead to the same total flow through a uniform liner as in the actual liner;
k_G = geometric average of hydraulic conductivities over the liner volume;
k_H = harmonic average of hydraulic conductivities over the liner volume;
k_i = geometric average of hydraulic conductivities over the ith element (having volume V_e);
n = number of elements in the FE model;
n_{par} = number of parameter sets considered in the simulation;
n_{sim} = number of simulations used to estimate statistics of each parameter set;
Q = total flow through the spatially random soil liner;
Q_{μ_k} = total flow through a soil liner having spatially uniform hydraulic conductivity equal to μ_k;
V = total volume of the soil liner = $X \times Y \times Z$;
V_e = element volume over which geometric averaging takes place = $\Delta z \times \Delta y \times \Delta z$;
X = liner thickness;
x = spatial coordinate in three dimensions;
Y = liner plan dimension;
Z = liner plan dimension perpendicular to Y and assumed equal to Y;
α_μ = regression coefficient used in the prediction of $\mu_{k_{\text{eff}}}$;
α_σ = regression coefficient used in the prediction of $\sigma_{k_{\text{eff}}}$;
γ, $\gamma_{\ln k}$ = variance reduction functions when averaging $\ln k$ over some volume;
Δx = X-direction dimension of geometrically averaged element;
Δy = Y-direction dimension of geometrically averaged element;
Δz = Z-direction dimension of geometrically averaged element;
θ_i = directional correlation length of the $\ln k$ random field in the ith direction, $i = 1, 2, 3$;
$\theta_{\ln k}$ = correlation length of the $\ln k$ random field;
μ_k = mean of the hydraulic conductivity field k;
μ_{k_A} = mean of the arithmetic averages of element geometric averages k_i over the liner volume;
$\mu_{k_A j}$ = mean of the arithmetic averages of element geometric averages k_i over the liner volume for the jth parameter set;
$\mu_{k_{\text{eff}}}$ = mean of effective hydraulic conductivity k_{eff};
μ_{k_G} = mean of the geometric average of the hydraulic conductivity over the liner volume;

J. Geotech. Geoenviron. Eng. 2013.139:937-946.

$\mu_{k_{Gj}}$ = mean of the geometric average of the hydraulic conductivity over the liner volume for the jth parameter set;
$\widehat{\mu}_{k_{\text{eff}j}}$ = sample mean of the effective hydraulic conductivity from the simulation runs for the jth parameter set;
$\mu_{\ln k}$ = mean of log-hydraulic conductivity field $\ln k$;
$\mu_{\ln k_{\text{eff}}}$ = mean of the log-effective hydraulic conductivity;
ξ = ratio of liner thickness X to plan dimension $\sqrt{YZ}$;
ξ_j = ratio of the liner thickness to plan dimension for the jth parameter set;
$\rho_{\ln k}$ = correlation coefficient between two points in the $\ln k$ random field;
σ_k = SD of hydraulic conductivity field k;
σ_{k_A} = SD of the arithmetic averages of element geometric averages k_i over the liner volume;
σ_{k_Aj} = SD of the arithmetic averages of element geometric averages k_i over the liner volume for parameter set j
$\sigma_{k_{\text{eff}}}$ = SD of effective hydraulic conductivity k_{eff}
σ_{k_G} = SD of the geometric average of the hydraulic conductivity over the liner volume;
$\sigma_{k_{Gj}}$ = SD of the geometric average of the hydraulic conductivity over the liner volume for the jth parameter set;
$\widehat{\sigma}_{k_{\text{eff}j}}$ = sample SD of the effective hydraulic conductivity from the simulation runs for the jth parameter set;
σ_{k_i} = SD of the geometric average of the hydraulic conductivity field over the ith element;
$\sigma_{\ln k}$ = SD of log-hydraulic conductivity field $\ln k$;
$\sigma_{\ln k_{\text{eff}}}$ = SD of the log-effective hydraulic conductivity;
τ = distance between two points in the liner;
τ_i = distance between two points in the liner in the ith direction, $i = 1, 2, 3$;
v_k = coefficient of variation of hydraulic conductivity k;
$v_{k_{\text{eff}}}$ = coefficient of variation of effective hydraulic conductivity k_{eff}; and
Φ = standard normal cumulative distribution function.

References

Benson, C. H. (1993). "Probability distributions for hydraulic conductivity of compacted clay liners." *J. Geotech. Eng.*, 119(3), 471–486.

Benson, C. H., and Charbeneau, R. J. (1991). "Reliability analysis for time of travel in compacted soil liners." *Proc., Geotechnical Engineering Congress, Geotechnical Special Publication No. 27*, F. G. McLean, D. A. Harris, and D. W. Harris, eds., ASCE, Reston, VA, 456–467.

Benson, C. H., and Daniel, D. E. (1994a). "Minimum thickness of compacted soil liners: I. Stochastic models." *J. Geotech. Eng.*, 120(1), 129–152.

Benson, C. H., and Daniel, D. E. (1994b). "Minimum thickness of compacted soil liners: II. Analysis and case histories." *J. Geotech. Eng.*, 120(1), 153–172.

Bogardi, I., Kelly, W. E., and Bardossy, A. (1990). "Reliability model for soil liner: Post construction." *J. Geotech. Eng.*, 116(10), 1502–1520.

Bouwer, H. (1969). "Planning and interpreting soil permeability measurements." *J. Irrig. And Drain. Div.*, 95(3), 391–402.

Byers, E., and Stephens, D. B. (1983). "Statistical and stochastic analyses of hydraulic conductivity and particle-size in a fluvial sand." *Soil Sci. Soc. Am. J.*, 47(6), 1072–1081.

Dagan, G. (1979). "Models of groundwater flow in statistically homogeneous porous formations." *Water Resour. Res.*, 15(1), 47–63.

Fenton, G. A., and Griffiths, D. V. (1993). "Statistics of block conductivity through a simple bounded stochastic medium." *Water Resour. Res.*, 29(6), 1825–1830.

Fenton, G. A., and Griffiths, D. V. (2008). *Risk assessment in geotechnical engineering*, Wiley, New York.

Freeze, R. A., and Cherry, J. A. (1979). *Groundwater*, Prentice Hall, Englewood Cliffs, NJ.

Griffiths, D. V., and Fenton, G. A. (1997). "Three-dimensional seepage through spatially random soil." *J. Geotech. Geoenv. Eng.*, 123(2), 153–160.

Gutjahr, A. L., Gelhar, L. W., Bakr, A. A., and MacMillan, J. R. (1978). "Stochastic analysis of spatial variability in subsurface flows: 2. Evaluation and application." *Water Resour. Res.*, 14(5), 953–959.

Liza, R. (2010). "Risk assessment of soil liners: Influence of correlation length." M.S. thesis, Civil Engineering Dept., Dalhousie Univ., Halifax, Canada.

Menzies, W. T. (2008). "Reliability assessment of soil liners." M.S. thesis, Civil Engineering Dept., Dalhousie Univ., Halifax, Canada.

Rogowski, A. S., Weinrich, B. E., and Simmons, D. E. (1985). "Permeability assessment in a compacted clay liner." *Proc., 8th Annual Madison Waste Conf.*, Dept. of Engineering Professional Development, Univ. of Wisconsin, Madison, WI, 315–337.

Smith, L., and Freeze, R. A. (1979). "Stochastic analysis of steady state groundwater flow in a bounded domain: 2. Two-dimensional simulations." *Water Resour. Res.*, 15(6), 1543–1559.

Vanmarcke, E. H. (1984). *Random fields: Analysis and synthesis*, MIT, Cambridge, MA.

Warren, J. E., and Price, H. S. (1961). "Flow in heterogenous porous media." *Soc. Pet. Eng. J.*, 1(3), 153–169.